



Cite this: *Polym. Chem.*, 2020, **11**, 6701

## Functional polyimides based on diamine containing diarylethylene moieties and their photochromic mechanism studies†

Wenxiu Huang,<sup>‡a</sup> Yubo Long,<sup>‡a</sup> Tengzhou Yang,<sup>a</sup> Zhuxin Zhou,<sup>ID a</sup> Lunjun Qu,<sup>ID a</sup> Minming Wu,<sup>\*a</sup> Xiaolong Qi,<sup>b</sup> Siwei Liu,<sup>ID a</sup> Zhenguo Chi,<sup>ID a</sup> Jiarui Xu<sup>a</sup> and Yi Zhang<sup>ID \*a</sup>

To expand the existing application conditions of photochromic polymers and enhance the tolerance of photochromic polymer electronic devices in extreme environments, a diamine monomer **DTEDA** bearing the diarylethylene (DTE) moiety was synthesized and polymerized with commercially available dihydrides to afford three polyimides (PIs, named **DTEODPI**, **DTE6FPI** and **DTEHPMPI**) through chemical imidization. These PIs realized reversible photo-triggered isomerization both in solution and in film state, with solution photoluminescence "on/off" effects. Semi-aromatic **DTEHPMPI** showed the largest contrast of color and fastest light response due to its local excited (LE) state. This research provides a simple method to prepare photochromic polymer materials with excellent comprehensive properties.

Received 29th July 2020,  
Accepted 28th September 2020

DOI: 10.1039/d0py01084g

rsc.li/polymers

### Introduction

Photochromic materials, which can be reversibly transformed into two isomers upon irradiation, might show significant differences in their physical and chemical properties, such as refractive index, absorbance, fluorescence intensity and dielectric constant under illumination.<sup>1</sup> Therefore, they have great potential in various practical applications such as data storage, optoelectronic devices, sensing, tunable self-assembly morphology, super-resolution microscopy, anti-counterfeiting materials and other fields.<sup>2–6</sup> Among the family of photochromes, including spiropyran,<sup>7</sup> azobenzene,<sup>8</sup> Schiff-base,<sup>9</sup> triarylethylene<sup>10–12</sup> and dithienylethene (DTE),<sup>13,14</sup> DTE is regarded as the shining star due to its inherent bistable characteristics and excellent recyclability. Although in-depth research has been conducted on small molecule DTE materials,<sup>15</sup> their poor thermal stability, inferior film-forming property and easy oxidation nature are still the key constraints;

however, by introducing DTE moieties into polymers, all issues can be resolved.<sup>16</sup>

Generally, there are two strategies for introducing DTE moieties into polymers: (1) doping DTE derivatives into polymers,<sup>17</sup> and (2) covalently incorporating DTE chromophores into the main or side chains of polymers.<sup>18</sup> The former method has obvious drawbacks, with low concentration doping influencing the photochromic properties while high concentration doping readily causes aggregation and phase separation due to low compatibility between DTE small molecules and polymer macromolecules.<sup>19</sup> The poor heat resistance of small molecule DTE dopants limits its application in the more demanding fields. Up to now, several kinds of DTE bonded functional polymer materials such as polycarbonate,<sup>20</sup> polysiloxane,<sup>21</sup> polyurethane<sup>22,23</sup> and other conjugated polymers<sup>24,25</sup> have been synthesized and investigated. Much progress in photochromic polymer materials has been made in terms of color changing speed and fatigue resistance,<sup>26</sup> while other properties, such as high and low temperature resistance and extreme environmental resistance, have been neglected, and they are of great importance when put to practical use. To overcome the problems mentioned above, we considered combining DTE moieties with polymer materials possessing excellent properties. Compared with the polymers mentioned above, polyimides (PIs), as a family of functional polymer materials showing excellent intrinsic comprehensive performance, surpass other photochromic polymer materials in high glass transition temperature and high decomposition temperature, with superior film-forming properties, simple

<sup>a</sup>PCFM Lab, GD HPPC Lab, Guangdong Engineering Technology Research Centre for High-performance Organic and Polymer Photoelectric Functional Films, State Key Laboratory of Optoelectronic Materials and Technologies, School of Chemistry, Sun Yat-sen University, Guangzhou 510275, China. E-mail: wumm8@mail.sysu.edu.cn, ceszy@mail.sysu.edu.cn; Fax: +8620 84112222; Tel: +86 20 84112222

<sup>b</sup>Guangdong Hinnotech Co., Ltd, Jiangmen 529000, China

†Electronic supplementary information (ESI) available: Materials and instrument information, <sup>1</sup>H NMR, <sup>13</sup>C NMR and IR spectra, DSC curves, and the solubility of the polyimides. See DOI: 10.1039/d0py01084g

‡These authors contributed equally in this paper.

synthesis and easy mass production.<sup>27–30</sup> More importantly, PI could maintain its good performance even under extreme conditions. In addition, introducing DTE moieties into the polymer backbone would improve its quantum yield, which would help in improving its photochromic properties.<sup>20,31</sup>

Herein, three PIs (named **DTE6FPI**, **DTEHPMPI**, and **DTEODPI**) were prepared *via* chemical imidization, with a DTE containing diamine monomer **DTEDA** and three commercially available dianhydrides (**6FDA**, **ODPA**, and **HPMDA**). All three PIs are photochromic both in solution and in film state, with the colorless open-ring form turning into a red closed-ring form under ultraviolet (UV) light. The process is reversible when the red closed-ring form is irradiated with visible light and it turns to a colorless open-ring form. This is the first report on photochromic polyimides containing DTE moieties. The photochromic mechanism is speculated through theoretical calculations, and **DTEHPMPI** with a semi-aromatic structure had the fastest UV response and highest contrast color. The reversible photochromic property makes PIs advantageously applicable as UV sensors, anti-fake materials, smart windows, optoelectronic devices and many other fields.

## Results and discussion

### Synthesis and characterization of monomers

The diamine monomer **DTEDA** was obtained *via* a three-step synthesis route (Scheme 1) according to an earlier report.<sup>32</sup> The Friedel-Crafts acylation of **1** with glutaryl dichloride was performed in anhydrous CH<sub>2</sub>Cl<sub>2</sub> to obtain the colorless **Dione**. Afterwards the McMurry reaction was carried out to generate **DTE2Cl**, which can be functionalized using *n*-BuLi and tributyl borate in anhydrous THF, and the chlorine of **DTE2Cl** was sub-

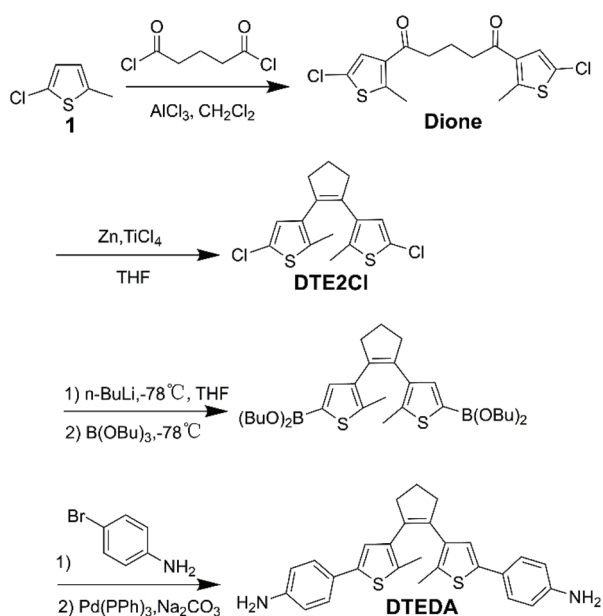
stituted by  $-B(OBu)_2$  to form an intermediate, which could react with 4-bromoaniline by Suzuki cross-coupling reaction to afford the desired diamine monomer **DTEDA**. The intermediates and product **DTEDA** were confirmed by <sup>1</sup>H NMR, <sup>13</sup>C NMR, IR and mass spectra, which are shown in the ESI.†

### Synthesis and characterization of polyimides

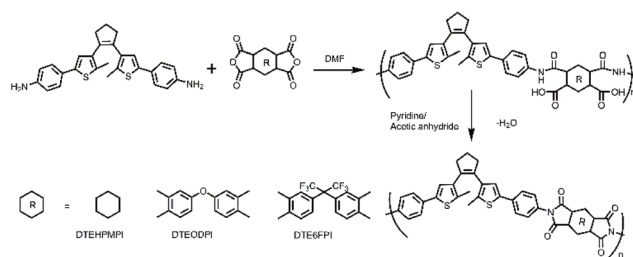
**DTEDA** was polymerized with three commercial dianhydride monomers 1,2,4,5-cyclohexanetetracarboxylic dianhydride (**HPMDA**), 4,4'-(hexafluoroisopropylidene)diphthalic anhydride (**6FDA**) and 4,4'-oxydiphthalic anhydride (**ODPA**) to prepare three PIs (**DTE6FPI**, **DTEHPMPI**, and **DTEODPI**). The preparation process of PIs is illustrated as follows. Equal molar amounts of **DTEDA** and dianhydride were mixed together in anhydrous dimethylformamide (DMF) and stirred at zero temperature to form viscous poly(amic acid) (PAA) solution, with solid contents of 15%–30%. Pyridine and acetic anhydride were added at room temperature to chemically convert PAAs into PIs. The solutions of PIs were subsequently poured into methanol to yield three novel PIs bearing DTE moieties (Scheme 2). As a result of complete imidization, the infrared absorption bands at 3500 cm<sup>-1</sup>–3300 cm<sup>-1</sup> belong to the N–H group of PAAs that disappeared, while the characteristic absorption peaks of the PI imide groups at about 1784 cm<sup>-1</sup>–1712 cm<sup>-1</sup> (C=O asymmetrical and symmetrical stretching) and 1353 cm<sup>-1</sup> (C–N–C stretching) arose. In addition, the stretching vibrations of the  $-CH_2$  and  $-CH_3$  groups assigned to the central cycloalkene ring clearly appeared at 2960 cm<sup>-1</sup>–2840 cm<sup>-1</sup>, which proved the successful introduction of the DTE group to the PIs. The intrinsic viscosities of **DTE6FPI**, **DTEHPMPI** and **DTEODPI** in NMP were 0.25 dL g<sup>-1</sup>, 0.18 dL g<sup>-1</sup>, and 0.73 dL g<sup>-1</sup>, respectively.

### Thermal properties

Thermal properties of PIs were investigated by thermogravimetric analyses (TGA) and differential scanning calorimetry (DSC), as shown in Table 1. These three PIs showed excellent thermal stability, with 5% weight loss temperatures ( $T_{d5\%}$ ) of 441 °C (**DTEHPMPI**), 492 °C (**DTE6FPI**) and 490 °C (**DTEODPI**) under N<sub>2</sub>, respectively. The aromatic imide structures made the  $T_{d5\%}$  of **DTE6FPI** and **DTEODPI** higher than that of **DTEHPMPI**. Based on the DSC curves, we found that all the PIs had a high glass temperature ( $T_g$ ), within the range of



Scheme 1 Synthesis routes of diamine monomers **DTEDA**.



Scheme 2 Synthesis routes of polyimides **DTEHPMPI**, **DTEODPI** and **DTE6FPI**.

**Table 1** Thermal properties of polyimide films

Polyimide	$T_g^a$	$T_d^b$	Char yield <sup>c</sup> (wt%)
DTE6FPI	306	492	44
DTEHPMPI	278	441	9
DTEODPI	295	490	35

<sup>a</sup> Measured by DSC at a heating rate of 10 °C min<sup>-1</sup>. <sup>b</sup> Measured by TGA at a heating rate of 20 °C min<sup>-1</sup> in nitrogen. <sup>c</sup> Residual weight percentage at 850 °C under N<sub>2</sub>.

250–280 °C (Fig. S3 in ESI†). Besides, good solubility in common solvents made them suitable for efficient and simple spin-coating, printing or roll-to-roll processing (Table S1 in the ESI†).

### Photochromic properties of polyimides

To assess the photochromic properties of PIs, UV-Vis experiments were conducted in NMP solution (Fig. 1) and in film state (Fig. 2) at room temperature. The absorption peaks in solution mainly appeared at 300 nm and 318 nm before

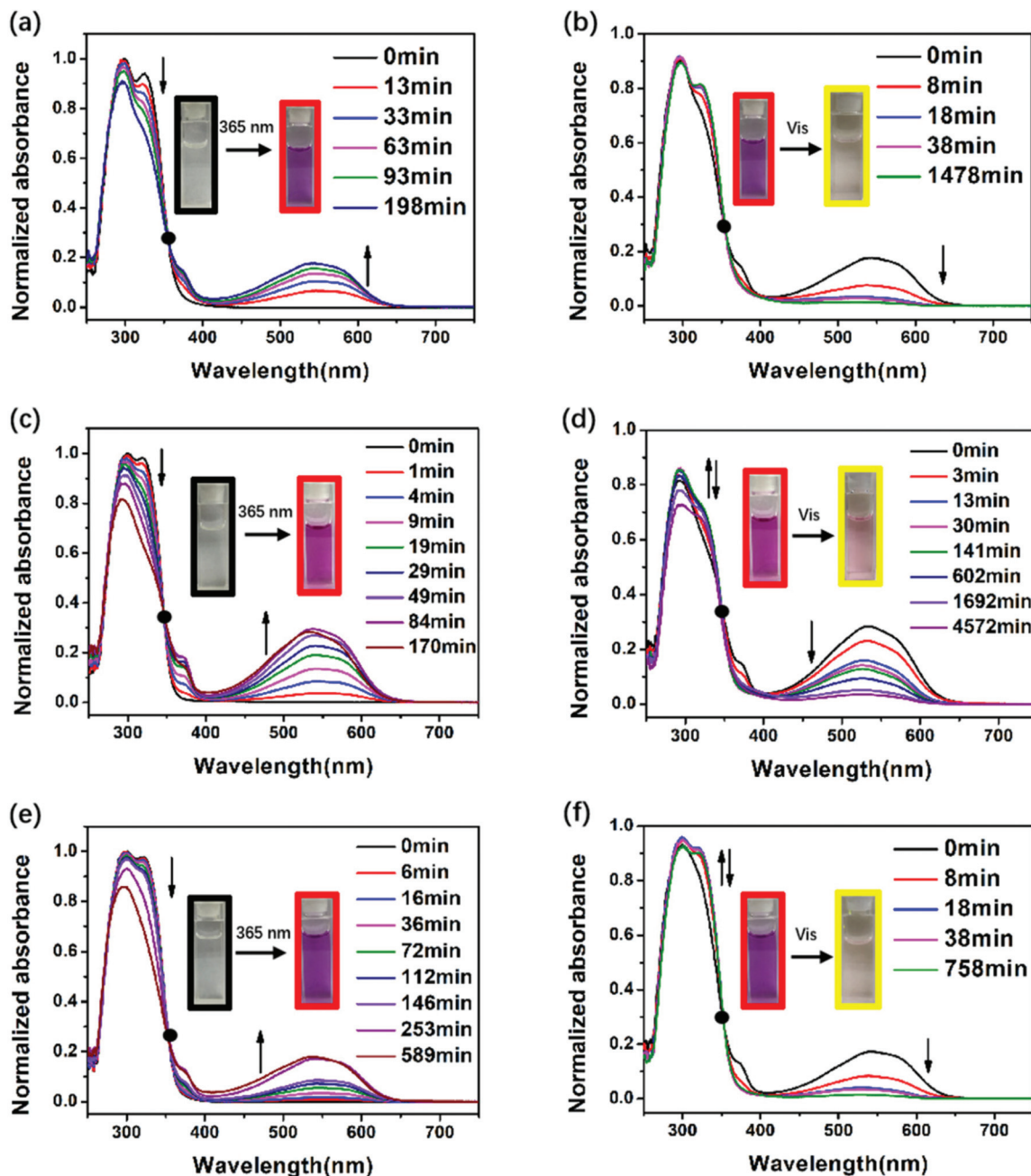


**Fig. 1** UV-Vis spectra of DTE6FPI (a and b), DTEHPMPI (c and d), and DTEODPI (e and f) in NMP solution (0.05 mmol L<sup>-1</sup>) during illumination with 365 nm UV light (a, c and e) or visible light (b, d and f).

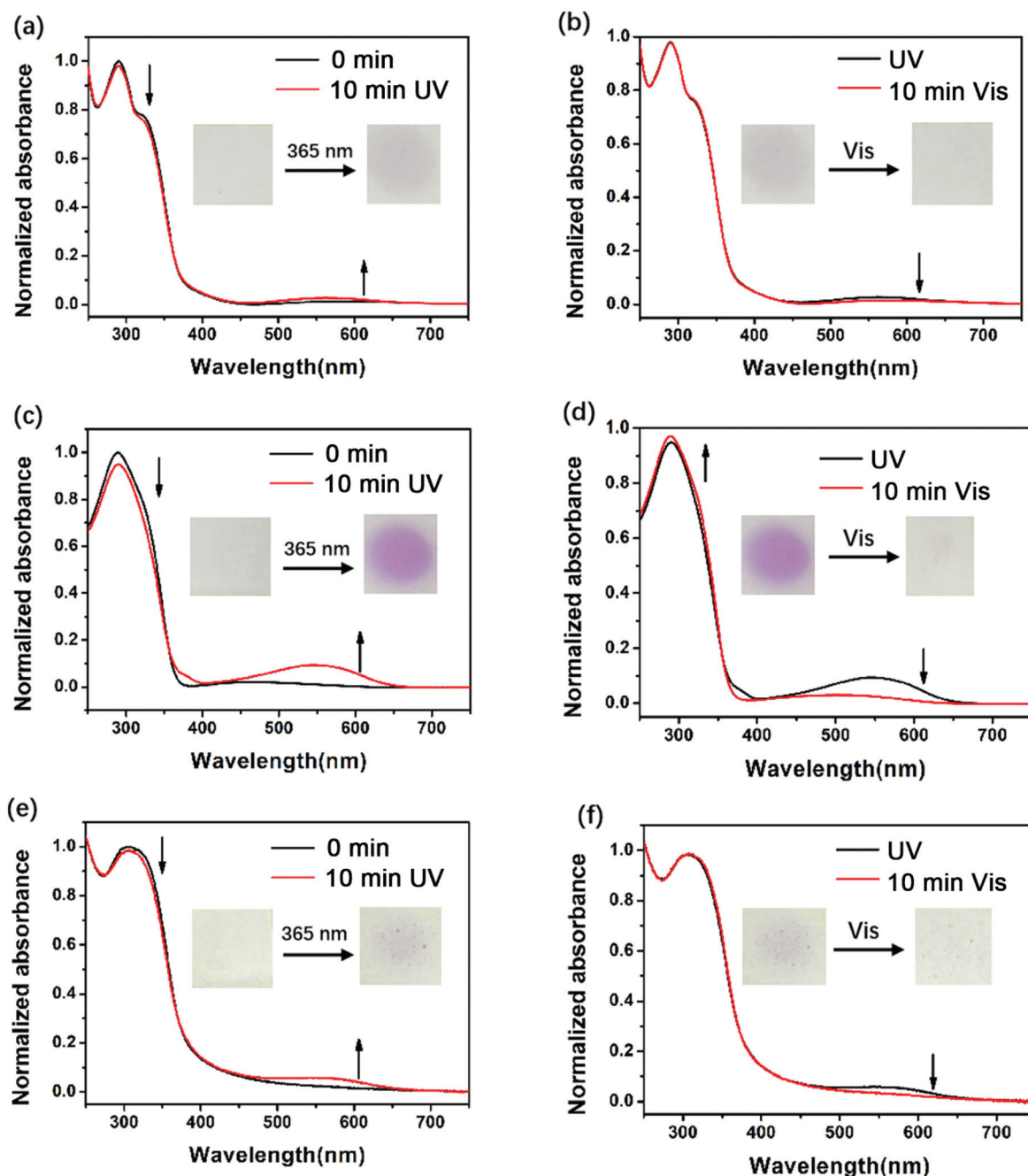


Fig. 2 UV-Vis spectra of DTE6FPI (a and b), DTEHPMPI (c and d), and DTEODPI (e and f) films during illumination with 365 nm UV light (a, c and e) or visible light (b, d and f).

irradiation. When exposed to 365 nm UV light, a new absorption peak in the visible region (540 nm) appeared and its intensity increased with time, accompanied by the decrease of the absorption peak in the short wavelength region (300 nm and 318 nm), changing the color from colorless to red. This can be attributed to the photoisomerization of DTE, which changed from an open-ring form to a closed-ring form under UV illumination, leading to larger conjugation and long wavelength light absorption. After irradiation for a period of time, the 540 nm peak no longer increases, indicating that the

photostationary state (PSS) is reached where two forms co-existed simultaneously in solution. Along with the UV-vis spectrum which showed an opposite change to the above results, the red solutions of the three PIs could be decolorized under visible light (>450 nm). The decolorization process proved that the closed-ring form could return to the initial open-ring form. It is noteworthy that a decrease in the short wavelength region (300 nm and 318 nm) was observed when they were exposed to visible light for longer than 38 min (DTE6FPI), 141 min (DTEHPMPI) and 38 min (DTEODPI). This phenomenon

might be due to the fact that partial ring-opened isomers absorbed a small amount of UV light that leaked from the filter and the ring-closing reaction occurred again. Nearly uniform absorption wavelengths of the open- and closed-ring forms were monitored for these PIs, demonstrating the negligible influence of the dihydrides on them. Fig. 2 shows the film state UV-Vis spectra, which clearly indicate that reversible photo-isomerization existed in film state as well, with similar spectra to their solution state spectra. The three DTE containing PI films exhibited the same behavior under 365 nm UV irradiation or visible light illumination as their solutions. As is shown in Fig. 2, DTEHPMPI had the largest contrast of color and fastest light response over DTE6FPI and DTEODPI.

### Photofluorescence switching behaviors of the polyimides

Fig. 3 exhibits the fluorescence spectra “on/off” switch of these three PIs in NMP, with intense emission peaks observed at 469 nm (DTE6FPI), 456 nm (DTEHPMPI), and 465 nm (DTEODPI), respectively. The fluorescence spectra were quenched upon irradiation with 365 nm UV light and almost returned to their initial intensity with visible light illumination (>450 nm). It is worth noting that there were significant spectral overlaps between the absorptions of closed-ring forms and emission of open-ring forms (Fig. 4). We assumed that the efficient energy transfer between the two isomers was responsible for this phenomenon. Due to the low detection limit of fluorescence intensity, we may use them as ultraviolet light sensors.

**Table 2** Theoretical analysis for model compounds

Compound	S1	Energy (nm/eV)	<i>f</i>
MO-DTE6F-O	H → L	520/2.39	0.0008
MO-DTE6F-C	H → L	803/1.54	0.0003
MO-DTEHPM-O	H → L	338/3.67	0.31
MO-DTEHPM-C	H → L	597/2.08	0.72
MO-DTEOD-O	H → L	500/2.48	0.0005
MO-DTEOD-C	H → L	754/1.64	0.0013

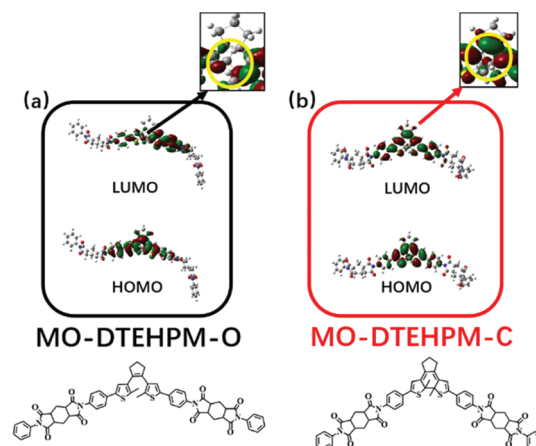


**Fig. 5** The frontier molecular orbitals of MO-DTEHPM-O (a), and MO-DTEHPM-C (b).

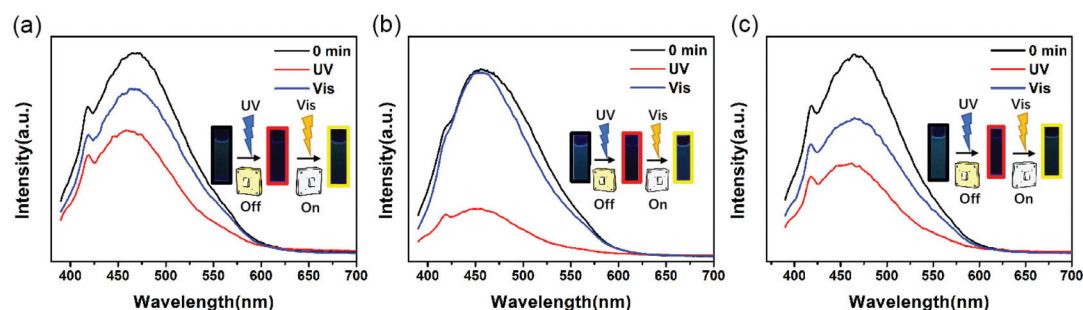


**Fig. 3** Change of emission spectra of DTE6FPI (a), DTEHPMPI (b), and DTEODPI (c) before irradiation (black line), after 365 nm irradiation (red line) and under visible light (blue line).

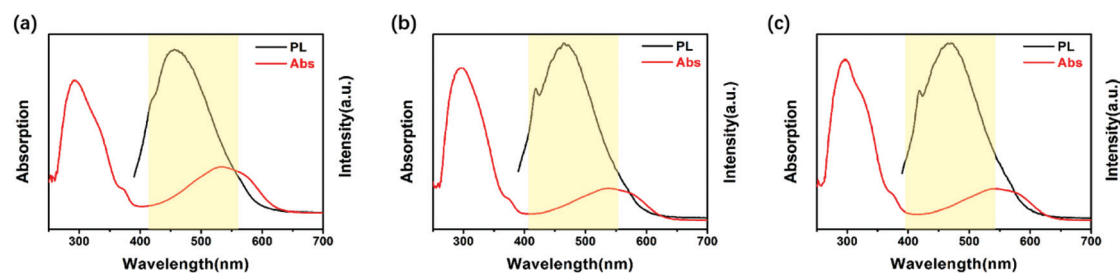


**Fig. 4** UV-Vis spectra of closed ring forms (red line) and emission spectra of open ring forms (black line) of DTE6FPI (a), DTEHPMPI (b), and DTEODPI (c).

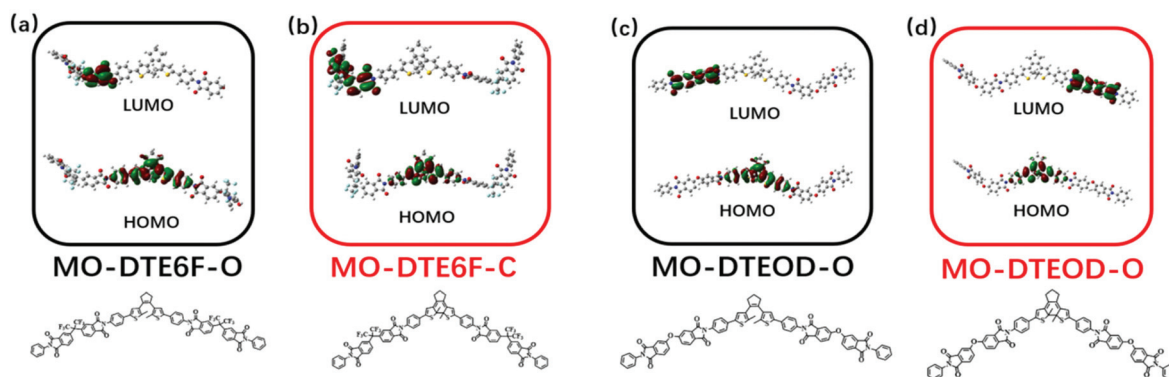


Fig. 6 The frontier molecular orbitals of MO-DTE6F-O (a), MO-DTE6F-C (b), MO-DTEOD-O (c), and MO-DTEOD-C (d).

### Theoretical analysis of the photochromic mechanism

To investigate the photochromic mechanism, we designed three model compounds (**MO-DTEHPM**, **MO-DTE6F**, and **MO-DTEOD**) according to the polymer repeating unit (Table 2). Their opening (O) and closed-ring (C) forms were optimized and calculated using time-dependent density functional theory (TD-DFT) for the frontier molecular orbitals with the Gaussian 09 program package. As we can see from Fig. 5, the highest occupied molecular orbital (HOMO) and lowest unoccupied molecular orbital (LUMO) of **MO-DTEHPM-O** were mainly concentrated around the DTE moiety and two benzene rings connected to thiophene. The first excited state ( $S_1$ ) is the transition from the HOMO to LUMO. The overlap of electron clouds between the two orbitals is large, and the oscillator strength ( $f$ ) is 0.31, which is a typical feature of the locally excited (LE) state and is beneficial for electron transition. The wave functions of activated carbon atoms on the LUMO are in the same phase (shown in red in Fig. 5a), indicating a tendency of forming a bonding orbital. Furthermore, the energy for the first excitation (338 nm) matched well with the experimental result (365 nm). So, we can deduce that **MO-DTEHPM-O** could absorb a 365 nm photon and transform into **MO-DTEHPM-C**. Similarly, the  $S_1$  of **MO-DTEHPM-C** presents an LE state (Fig. 5b). The activated carbon atoms in the HOMO show a bonding property while the LUMO is antibonding. It can be inferred that the electrons are excited from the HOMO to LUMO, and then **MO-DTEHPM-O** is formed. The photoisomerization of the aromatic structure (**MO-DTE6F** and **MO-DTEOD**) is shown in Fig. 6. The HOMO–LUMO separations showed that  $S_1$  is an intramolecular charge-transfer (CT) transition with small oscillator strength (0.0008 of **MO-DTE6F-O**, 0.0003 of **MO-DTE6F-C**, 0.0005 of **MO-DTEOD-O**, and 0.0013 of **MO-DTEOD-C**). The above results indicate that the semi-aromatic structure is more beneficial for energy absorption and the occurrence of photoisomerization.

## Conclusions

In this article, we reported the synthesis of a symmetrical diamine **DTEA** containing DTE *via* a three-step procedure

and polymerization with three commercial dianhydrides to afford three PIs (**DTEODPI**, **DTE6FPI**, and **DTEHPMPI**). All three PIs realized reversible photo-triggered isomerization both in solution and in film state, with photoluminescence “on/off” effects in solution. Among them, the semi-aromatic **DTEHPMPI** polymer had the largest contrast of color and fastest light response due to its LE state electron distribution over the DTE fragment. The research provides a simple method to prepare photochromic polymer materials with excellent comprehensive properties.

## Experimental

Raw materials, synthesis route and instrumentation are presented in the ESI.†

## Author contributions

W. X. Huang, Y. B. Long, M. M. Wu and Y. Zhang conceived and designed the experiments. W. X. Huang, Y. B. Long, Z. X. Zhou, L. J. Qu, and X. L. Qi performed the experiments. All the authors were involved in the analyses and interpretation of data. W. X. Huang, Y. B. Long, and M. M. Wu wrote the manuscript with the help of Z. G. Chi, Y. Zhang, and J. R. Xu.

## Conflicts of interest

There are no conflicts of interest to declare.

## Acknowledgements

The financial support by the Science and Technology Project of Guangdong Province (No. 2015B090915003, 2019B040401002 and 2020B010182001), the National Natural Science Foundation of China (No. 51873239 and 51373204), the National 973 Program of China (No. 2014CB643605), and

the Leading Scientific, Technical and Innovation Talents of Guangdong Special Support Program (No. 2016TX03C295) is gratefully acknowledged.

## References

- 1 M. Irie, *Chem. Rev.*, 2000, **100**, 1685–1716.
- 2 H. Tian, *Angew. Chem., Int. Ed.*, 2010, **49**, 4710–4712.
- 3 B. Oruganti, P. P. Kalapos, V. Bhargav, G. London and B. Durbeej, *J. Am. Chem. Soc.*, 2020, **142**, 13941–13953.
- 4 N. Shao, J. Jin, H. Wang, J. Zheng, R. H. Yang, W. H. Chan and Z. Abliz, *J. Am. Chem. Soc.*, 2010, **132**, 725–736.
- 5 X. Y. Yao, T. Li, J. Wang, X. Ma and H. Tian, *Adv. Opt. Mater.*, 2016, **4**, 322–1349.
- 6 S. S. Wang, Y. Y. Zhou, L. L. Zhu, J. J. Zhang, Q. Zou, T. Zeng and W. B. Chen, *Chem. Commun.*, 2017, **53**, 9570–9573.
- 7 M. Suda, N. Takashina, S. Namuangruk, N. Kungwan, H. Sakurai and H. M. Yamamoto, *Adv. Mater.*, 2017, **29**, 1606833.
- 8 M. M. Lerch, M. J. Hansen, W. A. Velema, W. Szymanski and B. L. Feringa, *Nat. Commun.*, 2016, **7**, 12504.
- 9 E. Hadjoudis and I. M. Mavridis, *Chem. Soc. Rev.*, 2004, **33**, 579–588.
- 10 T. Yu, D. P. Ou, L. Y. Wang, S. Z. Zheng, Z. Y. Yang, Y. Zhang, Z. G. Chi, S. W. Liu, J. R. Xu and M. P. Aldred, *Mater. Chem. Front.*, 2017, **1**, 1900–1904.
- 11 T. Yu, Z. Y. Yang, T. G. Luan, Z. Mao, Y. Zhang, S. W. Liu, J. R. Xu, Z. G. Chi and M. R. Bryce, *Chem. Sci.*, 2016, **7**, 5302–5306.
- 12 L. Y. Wang, T. Yu, Z. L. Xie, X. J. Chen, Z. Yang, Y. Zhang, M. P. Aldred and Z. G. Chi, *J. Mater. Chem. C*, 2018, **6**, 8832–8838.
- 13 A. Peters and N. R. Branda, *Adv. Mater. Opt. Electron.*, 2000, **10**, 245–249.
- 14 Z. W. Zhang, J. J. Zhang, B. Wu, X. Li, Y. Chen, J. H. Huang, L. L. Zhu and H. Tian, *Adv. Opt. Mater.*, 2018, **6**, 1700847.
- 15 M. Herder, B. M. Schmidt, L. Grubert, M. Pätzelt, J. Schwarz and S. Hecht, *J. Am. Chem. Soc.*, 2015, **137**, 2738–2747.
- 16 R. Singh, H. Y. Wu, A. K. Dwivedi, A. Singh, C. M. Lin, P. Raghunath, M. C. Lin, T. K. Wu, K. H. Wei and H. C. Lin, *J. Mater. Chem. C*, 2017, **5**, 9952–9962.
- 17 O. Nevskiy, D. Sysoiev, J. Dreier, S. C. Stein, A. Oppermann, F. Lemken, T. Janke, J. Enderlein, I. Testa, T. Huhn and D. Wöll, *Small*, 2018, **14**, 1703333.
- 18 F. Stellacci, C. Bertarelli, F. Toscano, M. C. Gallazzi, G. Zotti and G. Zerbi, *Adv. Mater.*, 1999, **11**, 292–295.
- 19 J. Yang, Z. G. Chi, W. H. Zhu, B. Z. Tang and Z. Li, *Sci. China: Chem.*, 2019, **62**, 1090–1098.
- 20 H. Tian and H. Y. Tu, *Adv. Mater.*, 2000, **12**, 1597–1600.
- 21 J. Biteau, F. Chaput, K. Lahlil, J. P. Boilot, G. M. Tsvigoulis, J. M. Lehn, B. Darracq, C. Marois and Y. Lévy, *Chem. Mater.*, 1998, **10**, 1945–1950.
- 22 G. Pariani, R. Castagna, G. Dassa, S. Hermes, C. Vailati, A. Bianco and C. Bertarelli, *J. Mater. Chem.*, 2011, **21**, 13223–13231.
- 23 L. Oggioni, C. Toccafondi, G. Pariani, L. Colella, M. Canepa, C. Bertarelli and A. Bianco, *Polymers*, 2017, **9**, 462.
- 24 J. X. Bu, K. Watanabe, H. Hayasaka and K. Akagi, *Nat. Commun.*, 2014, **5**, 3799.
- 25 K. Watanabe, H. Hayasaka, T. Miyashita, K. Ueda and K. Akagi, *Adv. Funct. Mater.*, 2015, **25**, 2794–2806.
- 26 G. Pariani, M. Quintavalla, L. Colella, L. Oggioni, R. Castagna, F. Ortica, C. Bertarelli and A. Bianco, *J. Phys. Chem. C*, 2017, **121**, 23592–23598.
- 27 Y. W. Liu, Z. X. Zhou, L. J. Qu, B. Zou, Z. Q. Chen, Y. Zhang, S. W. Liu, Z. G. Chi, X. D. Chen and J. R. Xu, *Mater. Chem. Front.*, 2017, **1**, 326–337.
- 28 Z. X. Zhou, Y. Zhang, S. W. Liu, Z. G. Chi, X. D. Chen and J. R. Xu, *J. Mater. Chem. C*, 2016, **4**, 10509–10517.
- 29 Z. X. Zhou, W. X. Huang, Y. B. Long, Y. Q. Chen, Q. X. Yu, Y. Zhang, S. W. Liu, Z. G. Chi, X. D. Chen and J. R. Xu, *J. Mater. Chem. C*, 2017, **5**, 8545.
- 30 L. J. Qu, L. S. Tang, R. X. Bei, J. Zhao, Z. G. Chi, S. W. Liu, X. D. Chen, M. P. Aldred, Y. Zhang and J. R. Xu, *ACS Appl. Mater. Interfaces*, 2018, **10**, 11430–11435.
- 31 F. Liu, S. Bi, X. Wang, X. Leng, M. Han, B. Xue, Q. Li, H. Zhou and Z. Li, *Sci. China: Chem.*, 2019, **62**, 739–745.
- 32 C. M. Yu, B. C. Hu, C. Liu and J. T. Li, *J. Phys. Org. Chem.*, 2017, **30**, e3584, DOI: 10.1002/poc.3584.